Optimization of Pulsed Nd:YAG Laser Melting of Gray Cast Iron at Different Spot Sizes for Enhanced Surface Properties

A.R. Zulhishamuddin [1, a)] S.N. Aqida [1, 2, b)] and E.A. Rahim [3, c)]

[1]*Faculty of Mechanical Engineering, Universiti Malaysia Pahang, 26600, Pekan Pahang, Malaysia*
[2]*Automotive Engineering Centre, Universiti Malaysia Pahang, 26600, Pekan Pahang, Malaysia*
[3]*Faculty of Mechanical and Manufacturing Engineering, Universiti Tun Hussein Onn, 84600, Parit Raja, Batu Pahat, Johor, Malaysia*

[a)]*zulhishamuddin@yahoo.com*
[b)]*aqida@ump.edu.my*
[c)]*erween@uthm.edu.my*

Abstract. This paper presents a laser surface modification process of gray cast iron using different laser spot size with an aims to eliminate graphite phase and achieve minimum surface roughness and maximum depth of molten zone and microhardness properties. The laser processing was conducted using JK300HPS Nd:YAG twin lamp laser source pulse TEM_{00} mode, 50 W average power, 1064 nm wavelength and different laser spot sizes of 1.0 mm, 1.2 mm, 1.4 mm and 1.7 mm. Three controlled parameter were peak power (Pp), pulse repetition frequency (PRF) and traverse speed (v). Increasing spot size the parameter setting where peak power is increased and pulse repetition frequency and traverse speed is decreased. The modified surface of laser surface melting was characterized for metallographic study, surface roughness and hardness. Metallographic study and surface morphology were conducted using optical microscope while hardness properties were measured using Vickers scale. Surface roughness was measured using a 2D stylus profilometer. From metallographic study, the graphite phase was totally eliminated from the molten zone and formed white zone. This phenomenon affected hardness properties of the modified surface where maximum hardness of 955.8 $HV_{0.1}$ achieved. Optimization of laser surface modification was conducted for minimum surface roughness and maximum depth of modified layer and hardness properties. From the optimization, the higher desirability is 0.902. The highest depth of molten zone obtain from spot size 1.4 mm at 132 μm and the highest hardness is 989 $HV_{0.1}$ at laser's spot size 1.0 mm. The surface roughness increased when the spot size increased from 3.10 μm to 7.31 μm. These finding indicate potential application of enhanced gray cast iron in high wear resistance automotive components such as cylinder liner and break disc.

INTRODUCTION

Gray cast iron is a one of the engineering materials with wide range of applications and is used to manufacture automotive parts such as break disc, cylinder liner, cylinder head, engine block and gear box. Previous reports from industry and researches show that, these automotive parts usually experienced certain defects such as wear, corrosion and thermal fatigue. The operational conditions for these parts involved with high temperature, pressure and mechanical friction, which contribute to multifaceted, high-stress condition [1]. Failure of components made of gray cast iron occurred near-surface graphite phases acted as a source of crack nucleation under impact condition and caused crack growth. In automotive application, cylinder liner of engines experienced high friction at elevated temperature that requires such properties to prevent crack and to increase the life of cylinder liner. In long cycle operation high wear rate leads to corrosion and produce sulfur in the fuel during operation [2]. Therefore elimination of

ESAFORM 2016
AIP Conf. Proc. 1769, 030004-1–030004-6; doi: 10.1063/1.4963420
Published by AIP Publishing. 978-0-7354-1427-3/$30.00

graphite phase near the surface is an option. With the presence of hard phase on the surface, corrosion and wear can be avoided [3].

To date, various conventional and advanced processing methods have been used to produce hardened layer for high wear resistance including laser surface melting (LSM). This technique improves surface properties by formation of hard, homogenous and ultrafine structure of the material surface layer without changing its chemical composition [4]. This method has been proven to change the surface layer enhance surface hardness and wear resistance by elimination graphite on the surface [5 6, 7]. Previous report shows by modifying tool steel and low carbon steel surface, the material phase was transformed from ferrite to martensite and retained austenite [8 9].

The important processing parameters for the laser surface modification include laser beam power, laser spot size, heat intensity distribution across the beam, absorptivity of the beam energy by the treated material surface, scanning rate of the laser beam across the substrate surface and the thermal properties of the treated material [4]. Previous report shows that melting surface versus the intensity of energy will produce distinct linear relationship for melting zone, transformation zone and incipient melting at the surface followed by a predominantly transformed zone [10]. Although controlling laser power and traverse speed can melt the gray cast iron and increase the microhardness and modify the depth of the melting zone, however, little information was found on optimization of laser melting of gray cast iron at different laser spot sizes for maximum hardness properties and layer depth, and minimum surface roughness. At different spot sizes, parameters such as residence time, scan rate, PRF and energy density were varied corresponding to the preferred laser spot size to prevent material vaporization and irregular surface morphology [11]. The depth of the zone increases by increasing peak power and decreasing traverse speed and surface roughness were sharply decrease with the decreasing of peak power and increased traverse speed [12]. Meanwhile the increment of the laser beam size will reduce the laser irradiance and increase the residence time and also increase the grain diameter for H13 steels [11]. In this study, gray cast iron were processed at laser spot size at 1.0 mm, 1.2 mm, 1.4 mm and 1.7 mm. This investigation was conducted to optimize the laser processing in order to enhance the cylinder liner life and prevent premature failure of friction due to high temperature.

EXPERIMENTAL

As-received gray cast iron was cut into sample of 40 mm diameter and 10 mm thickness. Chemical composition of as-received gray cast iron show in Table 1. Figure 1 shows microstructure of as-received gray cast iron. The structure shows graphite lamella is surrounded with α-ferrite. Average hardness for this material is 278.5 $HV_{0.1}$. The laser processing was conducted using JK300HPS Nd:YAG twin lamp laser source pulse TEM_{00} mode, 50 W average power, 1064 nm wavelength and different laser spot size at 1.0 mm, 1.2 mm, 1.4 mm and 1.7 mm. To have different laser spot size the laser beam was defocused from its focal position to a focal position above the surface.

TABLE 1. Chemical composition for as-received gray cast iron.

Material	C	Si	Mn	P	S	Fe
Gray cast iron	3.55	1.58	0.76	0.09	0.08	Bal.

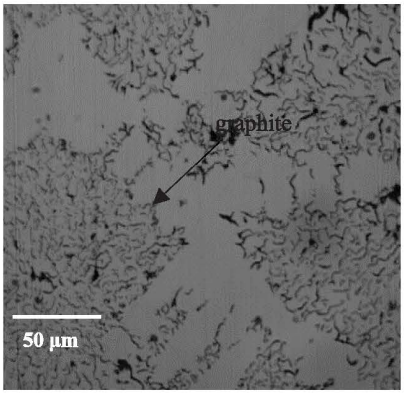

FIGURE 1. Microstructure as-received of gray cast iron at 500x magnification.

A full factorial design of experiment (DoE) of 3^3 was developed and yield 8 parameter for each different spot size. Controlled parameter were peak power (P_P), pulse repetition frequency (PRF) and traverse speed (v). Three responses were depth of molten zone, surface roughness and hardness. The parameter setting and outcome parameters are summarized in Table 2. The outcome parameters from the setting were pulse energy (E_P), residence time (T_R) and irradiance (I). Setting the parameter at different value will produce significant amount of energy and irradiance to melt the sample at different spot size. To prevent oxidation, laser processing was assisted by argon gas.

TABLE 2. Parameter settings for laser surface melting of gray cast iron.

Spot size (mm)	Parameter setting			Outcome parameter		
	P_P (W)	PRF (Hz)	v (mms^{-1})	E_P (J)	T_R (ms)	I (W/mm^2)
1.0	Low: 800 High: 1200	Low: 80 High: 90	Low: 19.2 High: 21.6	Low: 0.56 High: 0.63	Low: 1.9 High: 3.3	15.28
1.2	Low: 800 High: 1200	Low: 40 High: 50	Low: 13.6 High: 17	Low: 1.00 High: 1.25	Low: 2.9 High: 5.5	12.53
1.4	Low: 1500 High: 1800	Low: 15 High: 25	Low: 5.7 High: 9.5	Low: 2.00 High: 3.33	Low: 4.1 High: 8.2	8.82
1.7	Low: 2000 High: 2200	Low: 8 High: 11	Low: 2.4 High: 3.3	Low: 4.55 High: 6.25	Low: 12 High: 18	3.89

Modified layer thickness was measured using IM7000 Series Inverted Optical microscopes with Progress Capture 28.8 Jenoptik Optical System image analyzer software. The modified surface roughness was determined using 2D stylus profilometer. Hardness properties were measured using MMT Matsuzawa Vickers Hardness tester with 100 gf load. Experimental results were statistically analyzed by ANOVA approach to establish relationship between factors and responses. Optimization is to view minimize surface roughness and maximize the depth and hardness.

RESULT AND DISCUSSION

Surface morphology with corresponding cross sections of laser surface melting samples at different spot sizes is shown in micrographs of FIG. 2. The laser modified gray cast iron surface resulted in a graphite-free layer are as shown in micrograph (b) (d) (f) (h) of FIG. 2. Increasing laser spot size in gray cast iron influenced the sample surface morphology. The distance of laser pulse marks measured on the surface is shown on micrograph (a), (c), (e) and (g). Based on the micrographs, the radius of the laser mark was 0.84, 1.05 and 1.22 mm for respective spot size of 1 mm, 1.2 mm and 1.4 mm. Whereas the radius of laser pulse mark for spot size 1.7 mm was approximately 207 μm which overlapping at high percentage due to high energy range setting of 4.55-6.25 J. At the lower energy range of 0.56-3.33 J, the laser marks were 84 - 87.5% of the laser spot size. This was due to Gaussian beam effect which 86 % of the energy is contained at beam diameter that affect the surface [13]. The higher energy range melted 21% more area of the laser spot size though the irradiance was 3.89 W/mm^2. Besides, defocused spot sizes have shorter distance between material and nozzle, thus increased the laser mark size on sample surface. The structure of gray cast iron changed when the graphite flake was eliminated while the melting zone turned into white layer. This phenomenon is due to the localized rapid heating and cooling of the melted zone [14].

The surface morphology micrographs indicates the increment of laser spot size from 1.0 mm to 1.7 mm resulted the increasing of surface roughness. The maximum surface roughness increases from 3.9 μm to 8.3 μm. This is due to the increasing of residence time from 3.3 ms to 18 ms and the decreasing of irradiance from 15.28 W/mm^2 to 3.89 W/mm^2. From the cross-section micrographs, molten layer increases with the increment of the spot size. The maximum depth of the molten zone increases from 124 μm to 144 μm at spot size from 1.0 mm to 1.7 mm. The maximum layer depth can be obtained at spot size 1.7 mm with peak power 2000 W, PRF at 8 Hz and traverse speed at 2.4 mms^{-1}. The 1.7 mm spot size formed a larger area on the surface of the gray cast iron, absorbed the heat and penetrated into the sample surface. These results was found in laser melting of H13 steel, whereby the decreasing of irradiance and increasing of residence time produced bulging surface morphology [11]. In sample processed at 1.7 mm spot size, high peak power of 2000 - 2200 W emitted high energy of 4.55 - 6.25 J which travels deeper into the material's surface. The larger area of laser energy with longer laser beam-surface interaction time had caused the melted materials to reach higher temperature, which in turn leads to the further spreading of heat and deepening of the modified layer [15]. Besides that, high energy input distorted the surface morphology due to low viscosity of molten metal at high surface temperature. Lower surface roughness in sample processed at 1.0 mm spot size was due to low energy and high traverse speed which reduced the energy input to distort the surface morphology.

The increment of the depth of the molten zone by increasing the peak power and decreasing the traverse speed is a similar effect found by previous work on laser surface modification on H13 tool steel [12]. Furthermore, high thermal conductivity of gray cast iron allows high energy of 6.25 J to penetrate deeper at 144 μm on gray cast iron. Table 3 shows the range of layer's depth of the molten zone and surface roughness of laser melting samples at four different laser spot sizes. A thick layer of high hardness on the substrate surface can prolong cylinder liner life.

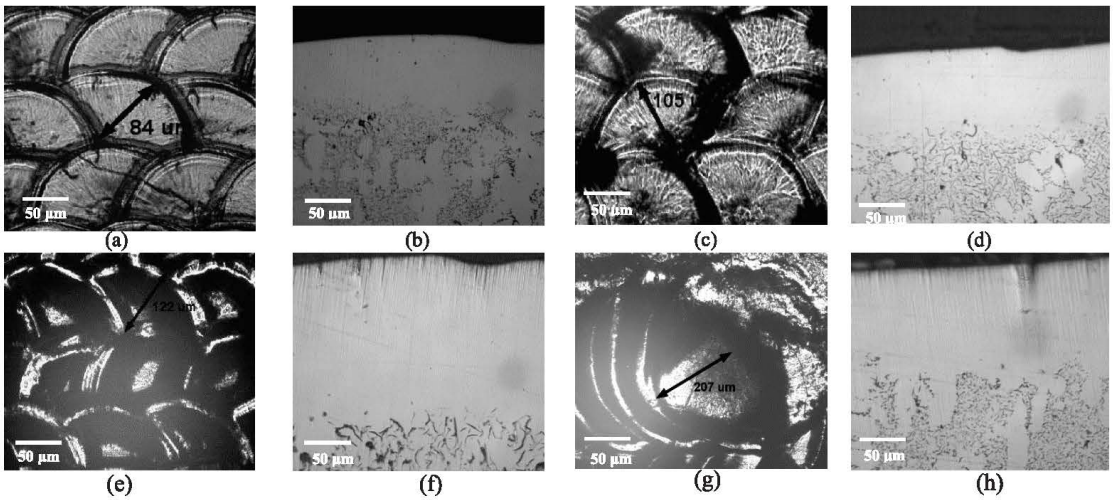

FIGURE 2. Surface morphology of samples processes at spot size 1.0 mm (a), (b); 1.2 mm (c), (d); 1.4 mm (e), (f) and 1.7 mm (g), (h).

TABLE 3. Surface roughness and depth of molten zone laser surface melting range at four different spot sizes.

Spot size (mm)	1.0	1.2	1.4	1.7
Ra (μm)	3.0-3.9	4.1-6.0	4.8-6.8	6.5-8.3
Depth ((μm)	42-124	62-128	55-132	40-144

The microhardness at the surface of gray cast iron increased from the substrate to the surface. From 1.0 mm spot size sample show average microhardness substrate increase from 307.4 $HV_{0.1}$ to 955.8 $HV_{0.1}$. Figure 3 show the microhardness graph and indention at the cross section for spot size 1.0 mm traverse from surface to the substrate. The increment of hardness was partly because of more carbon being dissolved in molten zone and changed the structure of austenite to martensite. Furthermore, high cooling rate causes austenite to crystallize as primary dendrites and comprising retained austenite as well as some martensite and cementite (Fe_3C) [14]. Insignificant hardness effect was analyzed from different spot sizes as the structure observed was similar in the micrographs of FIG 2. Laser processing at smaller spot size shows the higher hardness up to 975 $HV_{0.1}$ compared to bigger spot size at 732 $HV_{0.1}$.

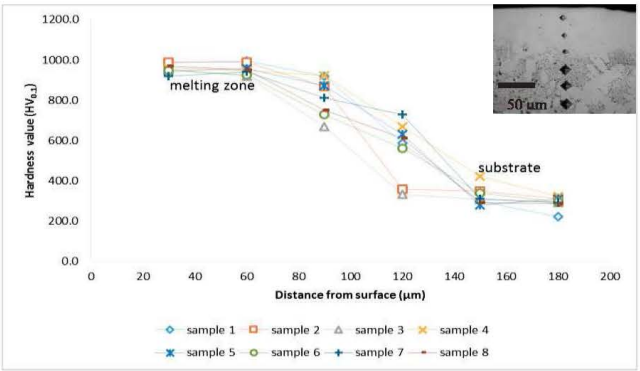

FIGURE 3. Hardness properties as a function of distance from surface in samples processed at 1.0 mm laser spot size.

The statistical analysis for hardness response indicates significant model for all spot sizes. Table 4 show ANOVA analysis for hardness response for spot size 1.0 mm. Based on the table, model F-value of less than 0.05 shows that the model is significant. All factors were significant with non-significant lack of fit. Analysis of other responses yield significant model.

TABLE 4. ANOVA analysis for hardness response for spot size 1.0 mm.

Spot size (mm)	Source	Sum of squares	df	Mean square	F value	p-value Prob>F	
	Model	4603.49	6	767.25	347.96	0.0410	significant
	A-Pp	994.58	1	994.58	451.06	0.0300	
	B-PRF	756.60	1	756.60	343.13	0.0343	
	C-v	233.28	1	233.28	105.80	0.0617	
1.0	AC	158.42	1	158.42	71.85	0.0748	
	BC	1452.60	1	1452.60	658.78	0.0248	
	ABC	1008.00	1	1008.00	457.15	0.0298	
	Residual	2.20	1	2.20			
	Cor Total	4605.70	7				

Optimization analysis was conducted to design an experiment within the given range of peak power, pulse repetition rate and traverse speed, with a view to minimize surface roughness and maximize depth of molten zone and hardness. The highest and lowest desirability are represent by 1 and 0 value respectively. The highest desirability value and parameter setting solution are listed in Table 5 and FIG.4 shows the contour plot of predicted for higher desirability for spot size 1.4 mm. It show the higher desirability 0.902 at spot size 1.4 mm and the lower desirability 0.686 at spot size 1.2 mm. Increasing spot size diameter will affect the laser parameter setting when the peak power is increased and pulse repetition frequency and traverse speed is reduced. At spot size 1.0 mm, 1.2 mm and 1.4 mm decreases the traverse speed shows effect to produce higher desirability. For spot size 1.7 mm higher traverse speed will produced higher desirability. Peak power, PRF and traverse speed show significant factor to optimize the surface of gray cast iron through laser processes.

TABLE 5. Processing parameter setting based on high desirability for spot size 1.0 mm, 1.2 mm, 1.4 mm and 1.7 mm.

Spot size	Peak power (W)	Pulse repetition frequency (Hz)	Traverse speed (mms^{-1})	Surface roughness (μm)	Depth (μm)	Hardness ($HV_{0.1}$)	Desirability
1.0	800	90	19.2	3.10	100	989	0.856
1.2	800	50	13.6	4.09	95	829	0.686
1.4	1800	15	5.7	5.49	132	935	0.902
1.7	2000	8	3.30	7.31	112	919	0.719

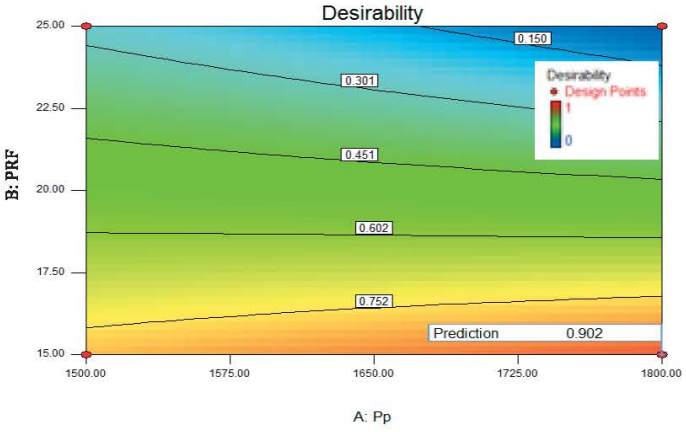

FIGURE 4. Counter plot of design for laser surface melting process optimization of gray cast iron at 1.4 mm laser spot size.

CONCLUSION

Laser surface melting using Nd:YAG laser system was conducted based on full factorial design of experiment (DoE) of 3^3 for gray cast iron. From metallographic study, the graphite phase was eliminated from the laser melting layer in all samples processed at four different spot sizes. The highest layer depth was measured in samples processed at 1.7 mm spot size where higher energy settings contribute to the molten layer depth. Increase of hardness was measured in molten layer up to three times of its substrate. The molten layer hardness range was 732 $HV_{0.1}$ to 955.8 $HV_{0.1}$. The smaller laser spot size of 1.0 mm yields lower surface roughness compared to larger spot sizes of 1.2, 1.4 and 1.7 mm. Optimization of laser parameters for minimum surface roughness and maximum hardness and molten layer depth shows the highest desirability factor of 0.902 for samples processed at 1.4 mm laser spot size. These findings signify parameters preference of laser melting of gray cast iron for enhanced surface properties.

ACKNOWLEDGMENTS

The authors would like to thank Universiti Malaysia Pahang for funding the research under project number GRS 140395 and to Universiti Tun Hussein Onn Malaysia who provide the research facilities.

REFERENCES

1. R. Ghasemi and L. Elmquist, Wear 317 (1–2), 153-162 (2014).
2. B.-Y. Jeong and M.-H. Kim, Surface and Coatings Technology 141 (2–3), 262-268 (2001).
3. J. Nadel and T. S. Eyre, Tribology International (1978).
4. J. Kusinski, S. Kac, A. Kopia, A. Radziszewska, M. Rozmus-Górnikowska, B. Major, L. Major, J. Marczak and A. Lisiecki, Bulletin of the Polish Academy of Sciences: Technical Sciences 60 (4) (2012).
5. X. Cheng, S. Hu, W. Song and X. Xiong, Vacuum 101, 177-183 (2014).
6. M. Paczkowska, Archives of Mechanical Technology and Automation 32 (1) (2012).
7. Z. k. Chen, T. Zhou, P. Zhang, H.-f. Zhang, W.-s. Yang, H. Zhou and L.-q. Ren, Optics & Laser Technology 72, 15-24 (2015).
8. A. Amirsadeghi, M. H. Sohi and S. F. K. Bozorg, Journal of Iron and Steel Research International 15 (4), 85-94 (2008).
9. A. Blarasin, S. Corcoruto, A. Belmondo and D. Bacci, Wear 86, 315-325 (1983).
10. J.-H. Hwang, Y.-S. Lee, D.-Y. Kim and J.-G. Youn, Journal of Materials Engineering and Performance 11 (3), 294-300 (2002).
11. S. N. Aqida, S. Naher and D. Brabazon, in *14th International ESAFORM Conference on Material Forming* (Queen's University Belfast, Northern Ireland, United Kingdom, 2011), Vol. 1353, pp. 1081-1086.
12. F. Fauzun, S. N. Aqida, M. S. Wahab and W. Saidin, Advanced Materials Research 1024, 215-218 (2014).
13. I. B. Allemann and J. Kaufman, Basics in Dermatological laser Applications 42, 7-23 (2011).
14. K. Y. Benyounis, O. M. A. Fakron, J. H. Abboud, A. G. Olabi and M. J. S. Hashmi, Journal of Materials Processing Technology 170 (1-2), 127-132 (2005).
15. Z.-k. Chen, T. Zhou, R.-y. Zhao, H.-f. Zhang, S.-c. Lu, W.-s. Yang and H. Zhou, Materials Science and Engineering: A 644, 1-9 (2015).